Journal of Biomedical Optics 8(1), 80–86 (January 2003)

Measurement of skin stretch via light reflection

Nejat Guzelsu
University of Medicine and Dentistry of New Jersey-SOM
Biomechanics Lab.
and
Rutgers University Bioengineering Program
Tr#4, 675 Hoes Lane
Piscataway, New Jersey 08854

John F. Federici
New Jersey Institute of Technology
Department of Physics
University Heights
Newark, New Jersey 07102

Hee C. Lim
New Jersey Institute of Technology
Department of Physics
University Heights
Newark, New Jersey 07102

Hans R. Chauhdry
New Jersey Institute of Technology
Department of Mathematics
University Heights
Newark, New Jersey 07102

Art B. Ritter
University of Medicine and Dentistry of New Jersey-NJMS
Department of Physiology
University Heights
Newark, New Jersey 07103

Tom Findley
University of Medicine and Dentistry of New Jersey-SOM
Department of Physical Medicine and Rehabilitation
Stratford, New Jersey 08084

Abstract. A noninvasive technique for measuring the stretch of skin is described. The technique utilizes changes in the reflectivity of polarized light intensity as a monitor of skin stretch. Measurements of *in vitro* pigskin and *in vivo* human skin show that the reflectivity of polarized light intensity increases linearly with stretch. The changes in diffusive reflectivity properties of skin result from the alterations that take place in the roughness across the thickness of the skin layers due to stretch. Conceptually, as the roughness of a layer decreases with stretch, a smoother reflecting media is produced, resulting in a proportional increase in the specular reflection. Results can be easily extended to a real-time stretch analysis of large tissue areas that would be applicable for mapping the stretch of skin. [DOI: 10.1117/1.1527936]

Keywords: polarization imaging; skin roughness; skin stretch; light reflection.

Paper JBO 01020 received Mar. 28, 2001; revised manuscript received Mar. 26, 2002 and July 10, 2002; accepted for publication July 17, 2002.

1 Introduction

Visualization of skin deformations due to different surgical procedures is an important problem in plastic surgery. Large local deformations can be easily produced during suturing. Locally generated large deformations during the skin expansion and skin flap procedures can create undesirable consequences. Deformation of the skin is related to the mechanical forces that are generated in the skin due to external and/or internal forces. High-tension forces that can generate local large deformations across a sutured wound are likely to produce a stretched hypertropic scar at that site.[1,2] Better scars are produced when the wound axis is placed parallel to Langer's lines (tension) compared to the case when the axis is across the lines.[1,3] Dehiscence, ischemia, or necrosis may be expected in regions of high stresses through compromise of circulation in the subdermal vascular plexus. Blood flow is inversely proportional to wound closure tension, as observed in animal studies.[4] Therefore, it is worthwhile to determine deformations and estimate stresses in skin tissue accurately for a given pattern of wound suturing and/or in other surgical procedures where the large stretches are generated in skin.

Biomechanical models and finite element analysis have been used in skin research to compute large stretches and predict stress concentrations. Using this information, researchers have determined preferred suturing patterns and wound geometries.[5–8] Also, finite element analysis has been applied to deformation patterns and to estimate the stress distributions in skin flaps.[9] Note here that the deformation patterns *in vivo* situations will only help to estimate the stresses in skin because of skin's anisotropic mechanical properties,[7,10,11] and also the interaction between the dermis and hypodermis.[12]

In vivo surface deformation patterns of skin can be obtained optically by a video dimension analyzer (VDA) or video motion analyzer (VMA) (Refs. 13, 14, and 15). The VDA system consists of a TV camera, a monitor, and a dimensional analyzer. The dimensional analyzer converts the distance between parallel stain markers on the surface of a substrate under investigation to a proportional voltage. VMA

Address all correspondence to Nejat Guzelsu, Dept. of Osteosciences/Biomechanics, PCC Suite 102, 40 East Laurel Road, Stratford, New Jersey 08084-1504. Tel: 856-566-2731; Fax: 856-566-2733; E-mail: guzelsu@umdnj.edu

1083-3668/2003/$15.00 © 2003 SPIE

systems can generate a 3-D image of stretch using fluorescent markers (or other physical markers) that are placed on a tissue under study. The markers are imaged with three different cameras and the information is stored in a computer. The stretches can be computed from the two successive video frame informations via software.

Optical properties of skin and reflection of light from the skin surface and the interior layers of skin have been investigated.[16] In this paper, an optically based noncontact, *in situ* technique for measuring skin stretch is reported. This optical technique[17] is based on changes in the reflectivity of polarized light as the skin is stretched. As the skin is stretched, the roughness of the tissue is reduced, resulting in a smoother reflecting surface and a commensurate increase in the polarized reflected light. A simple model of surface roughness predicts[17] that the reflectivity should vary linearly with stretch as is observed experimentally. Several groups have used the reflection of polarized light to image tissues such as skin.[18–23] In using polarized light, one can take advantage of the fact that linearly polarized light becomes increasingly randomly polarized as it propagates through the skin due to its large scattering coefficient. Linearly polarized light with cross polarizers has been used in lens photography to investigate the skin surfaces and to improve anterior segment photography.[19–23] Light that is reflected from the skin has two components. The first one, which maintains the polarization of the incident light, is the regular reflectance that comes predominately from the surface of the skin. The second component comes from within the tissue due to backscattering of light from the various skin layers. The backscattered light is predominately randomly polarized due to the large scattering coefficient of the skin. Using a polarized light source and another polarizer in front of the camera parallel to first polarizer (in front of the light source), researchers observed skin surface details from the reflected light (surface reflection). In cross-polarization they eliminate the surface reflection and preferentially detect the diffusely backscattered light. From the backscattering light reflection they obtain information about pigmentetion, erythema, infiltrates, vessels, and other intracutaneous structures.

Our previous experimental studies on guinea pigs and the theoretical modeling suggest that changes in the roughness of the skin layers may be responsible for the observed dependence of reflectivity on stretch.[17] In this paper, we discuss the experimental setup and the measuring technique in addition to preliminary data obtained from animal and *in vivo* human skin experiments.

2 Measurements

2.1 Experimental Technique

The polarization properties of reflected or transmitted light depend on the number of scattering events that take place for each photon.[18] For photons that suffer virtually no scattering events (so-called ballistic photons), the polarization properties are preserved. As photons participate in more and more scattering events, the final polarization state becomes more randomized. In the limit of many scattering events in a turbid tissue such as skin, the outgoing photons (diffusive photons) are unpolarized with equal intensity components parallel and perpendicular to the polarization of the incident light. Although the diffusive photons can provide information along the tissue's thickness (depending on the penetration depth of the light source), it is difficult to determine which areas of tissue were sampled due to the multiple scattering events. On the contrary, ballistic photons are partially reflected whenever there is an index of refraction difference from one tissue layer into another. Hence, the diffusive photons generally contribute to a background noise in every direction, which masks the tissue imaging information carried by the ballistic photons. In the 2-D polarization imaging technique[18] as well as other similar polarization measurements,[19,22] the perpendicular component of diffusely reflected light is subtracted from the parallel component (ballistic plus diffusive) to remove the background noise.

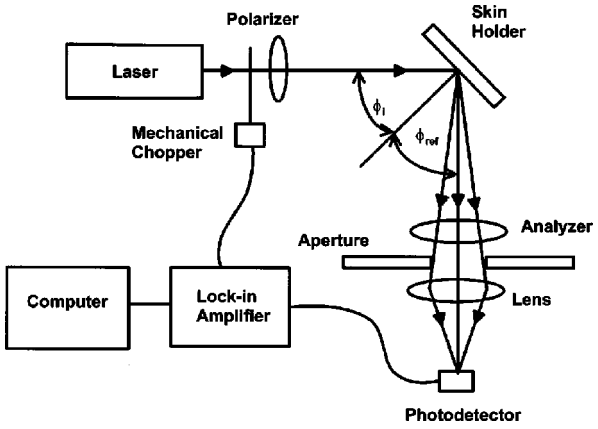

Fig. 1 Experimental setup. Laser light is reflected from the middle portion of the skin sample where the stretch field is uniform. An angle of incidence (ϕ_i) of 45 deg is used. Polarizer and analyzer are polarizing filters for the incident and reflected light, respectively. The reflected light from the skin sample is collected onto the photodetector using a lens after it passes through the analyzer. The solid angle of collection is about 2.5×10^{-2} sr.

The reflected power in both the parallel and perpendicular polarization is measured as a function of the incident light polarization and skin stretch. The experimental setup for measuring changes that take place in the light intensity due to applied skin stretch is shown in Figure 1. A He-Ne laser ($\lambda = 632.8$ nm, $P \leqslant 0.25$ mW) is used as a light source. Linearly polarized light is reflected from the surface of the skin. The light intensity is kept low enough to ensure a linear detector response (voltage proportional to laser power) and to protect the skin from damage. The angle of incidence in this study was $\phi_i = 45$ deg. The diameter of the incidence light was adjusted to 2 mm. The reflected light is collected onto the single-element silicon photodetector using a lens ($f = 35$ mm) after it passes through a second polarizer (analyzer). To within our limits of detection, the photodetector is polarization insensitive. The polarization of the incident light and the analyzer can be set in one of two perpendicular orientations: either parallel or perpendicular to the plane of incidence. The plane of polarization of light emerging from the laser is at 45 deg with respect to the first polarizer. This ensures equal intensities in either plane of polarization that is incident on the sample. The laser power is detected using the silicon photodetector by mechanically chopping the incident laser light and utilizing a lock-in amplifier and standard

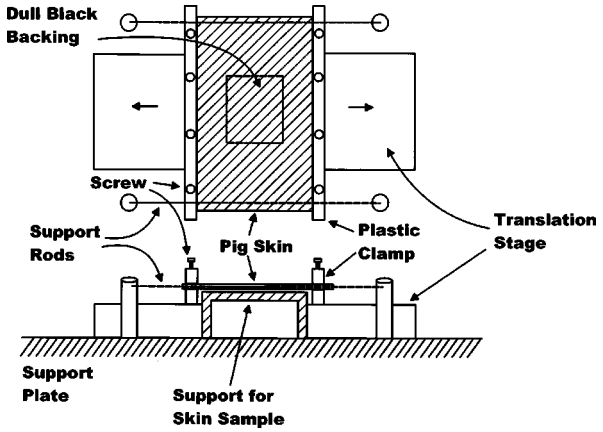

Fig. 2 Skin stretch device. Skin piece is attached to the computer-controlled translation stages via plastic clamps. Both stages are translated equal distances. This enables us to create a uniform stretch at the center of the skin sample where the polarized laser light is reflected. Support rods, which pass through the side holes of the skin sample, prevent the center of the skin from contracting, and moving toward the center of the skin stretch device.

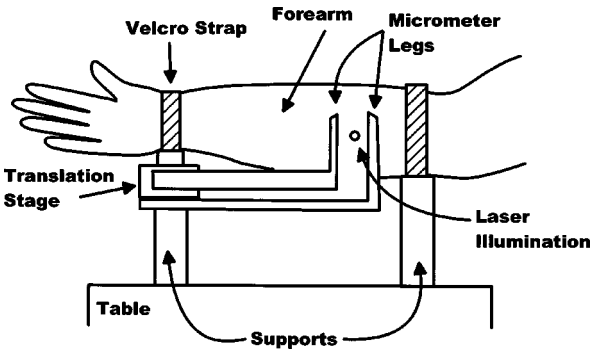

Fig. 3 Forearm is rested on the supports. Velcro straps stabilize the forearm. A computer-controlled translation stage is secured on to the left support. One of the micrometer legs is rigid while the other is translated by the stage. The legs of the micrometer are attached to the skin of the forearm with a double-sided Scotch tape with an initial 57-mm opening.

phase-sensitive detection techniques. In this technique, the laser power on the skin is modulated at a fixed frequency by alternatively blocking and unblocking the laser beam with a rotating slotted disk. Consequently, the optical signal measured by the detector is modulated at this same frequency. The lock-in amplifier is designed to eliminate noise at all frequencies while locking onto and amplifying the signal frequency. This technique is particularly useful when measuring small signals in the presence of large background noise.

2.2 Materials and Methods

In vitro experiments were performed on pigskin samples taken from the animals' shoulders. Pigskin samples were obtained from a local slaughter house. A simple device was built to apply stretch to the skin piece, as shown in Figure 2. Two opposite sides of the square (70×70 mm) skin sample were attached to the computer-controlled translation stages using plastic clamps. The distance between the clamps is 57 mm. The other sides of the sample were run through a metal cylindrical rod via 2-mm-diam holes that were punched along the sides of the sample. When the skin was stretched an equal amount with the translation stages, these rods prevented the center of the skin from contracting and moving toward the center of the device (lateral contraction). The distance between the supporting cylindrical rods was 60 mm. The middle part of the Plexiglas plate was covered with a dull (nonshining) black thin plastic piece. This plastic piece eliminated any reflection from the Plexiglas surface. We obtained three samples from a single pigskin sample. The fatty tissue was completely removed from the backside of the samples. To obtain a repeatable data set, the pig spine orientation was used as an anatomical landmark. Square samples were taken from the skin piece where one side was taken parallel to the spine. The samples were placed such that the side of the square parallel to the spine was always parallel to the axis of the device where two translation stages are aligned. The samples were stretched parallel to the spine orientation and then back to the original position. During the experiments, the backside of the skin (the side facing the Plexiglas) was kept wet with saline solution (pH 7.4) to minimize the friction between the two materials and eliminate the drying of the skin.

Skin samples were stretched by equal displacement with the two computer-controlled translation stages. This enabled the center of the sample to be stationary with respect to the stretch device. Computer-controlled stepper motors were used to change the stretch of the skin in 100-μm steps. The stepper motors have a resolution of ±1 μm. During the measurements, laser light was reflected from this central portion of the skin. Various amounts of stretch, up to 17 mm (up to 12.3% of the unstretched length), were applied to the 57-mm skin span between the two clamps After the maximum stretch was reached, the skin sample was returned to its original position with the same protocol.

The measurement technique was tested on human skin *in vivo*. In this measurement, a special support for the right forearm was utilized. The experimental setup for holding the forearm is shown in Figure 3. As with the *in vitro* measurements, the stretch was computer controlled using a stepping motor. The forearm was supported with two plastic supports, one located under the wrist and the other one under the elbow. The arm was secured on these supports with Velcro straps. A micrometer was secured on one of the supports. The two legs of the micrometer were placed against the skin at the anterior side of the forearm. Two legs of the micrometer were attached to the skin of the forearm with a double-sided Scotch tape with an initial 57-mm opening. Intensities of parallel and perpendicular polarized light of the analyzer were measured. The differences of the reflected light intensities were plotted against the stretch relative to the initial length (57 mm). Data were recorded for stretch either along or perpendicular to the long axis of the forearm. Ten different subjects were tested. Some of the measurements were performed on different days and some of the measurement on the same day.

3 Results

When stretch is applied to samples of pigskin parallel to the spine, a nearly linear relation between the amount of stretch and normalized reflected light intensity is measured. Figure 4 shows a typical measurement using a He-Ne laser. The inci-

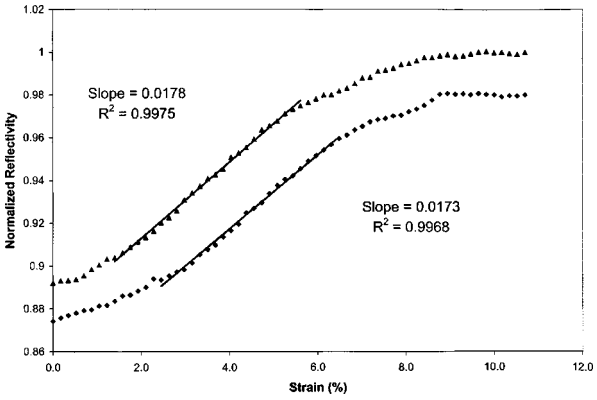

Fig. 4 Normalized reflectivity versus stretch for pigskin (shoulder) from two different animals. The bottom curve is offset by 0.02 for clarity. The initial stretching (below about 1.75 strain) removes sagging in the sample. The linear reflectivity versus stretch is observed for intermediate values of stretch. For large values of stretch, the reflectivity saturates. The straight lines are the best-fit linear regression lines to the data points.

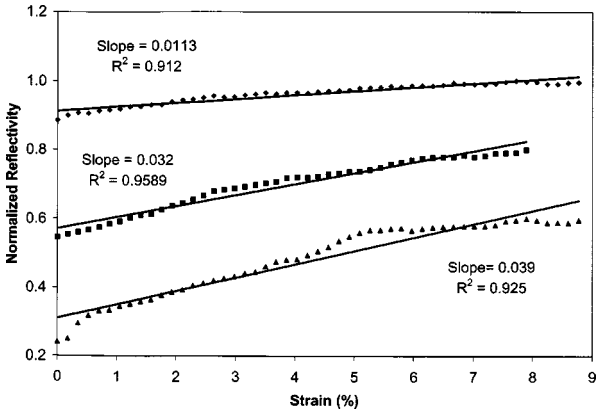

Fig. 5 Stretch versus reflected light intensity for *in vivo* human skin (Subjects 2, 7, and 9 top to bottom, respectively) for the anterior side of right forearm. For clarity, the data for subjects 7 and 9 are shifted down by 0.2 and 0.4, respectively. The solid lines are the best-fit linear regression fits to the data.

dent light is polarized perpendicular to the plane of incidence and the spine direction (direction of applied load). Similar results were obtained for incident light polarized parallel to the plane of incidence and the direction of applied load. In plotting Figures 4, 5, and 6, we used the following strain measure ε $[\varepsilon=(L-L_0)/L_0]$, where L_0 and L stand for the length of the skin between the grips before and after the deformation, respectively. In Figure 4, the initial stretching (below about 1 mm; $\varepsilon=1.75\%$) removed sagging in the sample. The linear reflectivity versus stretch was observed for intermediate values of stretch. For large values of stretch, the reflectivity saturates. The straight line is the best-fit linear regression line to the data points. In our previous work, we developed a model[17] that predicts this linear behavior. In this model, the polarized reflectivity increases due to a reduction in surface roughness as the tissue is stretched.

The normalized reflected light intensity was computed by taking the difference between the two perpendicular components of the reflected light (the component parallel to the polarization of incident light minus the perpendicular component). The resulting number was then normalized to the maximum recorded value.

Similar results were obtained for *in vivo* human skin for the anterior side of right forearm. Before each measurement, any hair that might interfere with the measurements were shaved and each subject's skin was wiped with alcohol. Typical data is shown in Figure 5 for human subjects 2, 7, and 9, respectively. The solid lines are a least-squares linear fit to the data to determine the slope. The quality of the fit is indicated by the linear correlation coefficient (R^2) with a value of 1.0 indicating a perfectly linear set of data. The normalized reflected intensity is plotted against the additional stretch relative to the initial unstretched tissue (57 mm) (elongation of the distance from the original 57-mm opening). Table 1 summarizes the data for the 10 subjects. Note that while the slopes are different for the different subjects, the linear correlation coefficients indicate that all of the subjects' data is very well represented by a linear fit. As shown in Figure 6, as the stretch is increased further, the reflectivity saturates as indicated by the decreasing slope above stretches of 4 mm ($\varepsilon=7\%$) (Figure 4) and 5 mm ($\varepsilon=8.8\%$) (Figure 6).

To demonstrate the reproducibility of the measurement, the reflectivity versus stretch data were recorded on human subject 2 on the same bodily location for 10 different days. The experiments were preformed at the approximate same time of the day in a similar controlled environment (i.e., temperature, humidity). The subject was also allowed to rest and relax the skin surface for a consistent amount of time while the subject skin was treated with alcohol wipes between each measurement. It was found that the longer time intervals (>10 min) given between the cycles would reduce the effect of viscoelastic deformations and thus reduce the scatter in the data. On each day, 10 trials were conducted. The data are tabulated in Table 2. On to day-to-day basis, the data is reproducible to roughly 13%.

Table 1 Measured slope and corresponding linear correlation coefficient (R^2) for measurements on 10 different human subjects with various skin complexions, where the error in the average slope for each subject is below 13% and is determined by the standard deviation of the slope measurements.

Subject	Skin Complexion	Average Slope	Correlation Coefficient
1	Fair-white	0.0348	0.98700
2	Yellow	0.0103	0.99460
3	Yellow	0.0153	0.87780
4	Extreme white	0.0074	0.92368
5	Fair	0.0193	0.93604
6	Medium brown	0.0088	0.93970
7	Black	0.0321	0.95887
8	Light brown	0.0274	0.94131
9	Dark	0.0391	0.92500

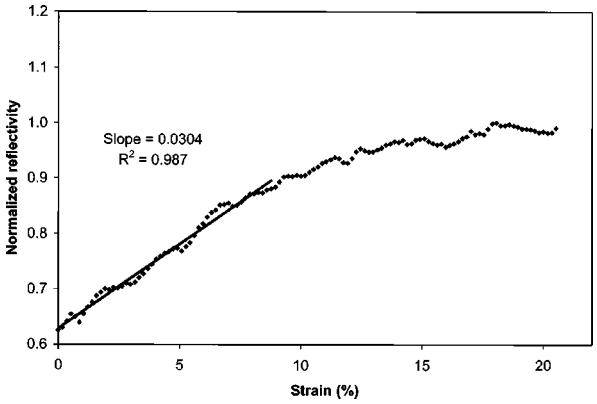

Fig. 6 Human forearm measurement for subject 1. For small values of stretch, the change in reflectivity is linear. As the stretch continues beyond about 8.8% strain, the reflectivity approaches a limit.

4 Discussion

In vivo human experiments on skin showed that the reflection properties of skin change with stretch for He-Ne wavelength ($\lambda = 632.8$ nm). Added linear regression lines showed that the intensity of the reflected specular light after subtracting the noise increases linearly with applied stretch (Figure 5). The slopes of the regression lines are different for different subjects (Table 1). Such differences are to be expected since the mechanical properties of tissue will vary with age, moisture content, and so on. However, it was reproducible for the same subject on different days under the same experimental conditions (Table 2).

The stretches in two perpendicular directions (parallel and perpendicular to the long axis of the forearm) yield good correlation between stretch and reflected light intensity and also it shows that skin has anisotropic properties which can be detected by light reflection (see Table 3). Similar stretch experiments on the volar surface of the forearm by other researchers showed that the mechanical properties of the forearm skin are anisotropic.[24,25] Also in that study it was shown that skin impressions that are taken by silicone rubber[26] changed with applied stretch. The linear relationship between applied stretch and polarized reflectivity can be understood and modeled if the skin surface is approximated by a sinusoidal curve in the resting stage. Stretching reduces its amplitude and increases its spatial scale, thereby making it smoother and flatter, resulting in a commensurate change in reflective characteristics of the skin.[17,25]

As the skin is stretched toward its maximum limit, one would expect the reflectivity to saturate with increasing stretch since its surface becomes mirror-like. Continued stretching will no longer increase the reflectivity at an appreciable level as compared to lower stress levels, since the surface is already as smooth as possible. This saturation is observed in latex membrane measurements.[17] The change in reflected light intensity is decreasing for larger stretches as evidenced by the reduction in the slope of the curve towards stretch distances larger than 5-mm stretch ($\varepsilon = 8.8\%$) for subject number 1 in Figure 6 and 4-mm stretch ($\varepsilon = 7\%$) in Figure 4. Similarly, this saturation behavior was observed by Ferguson and Barbenel[25] in their skin tension experiment in which skin behaved rather mechanically stiff in the direction perpendicular to the long axis of forearm as compare to parallel to long axis of forearm.

Table 3 Measured slope of reflectivity versus stretch data for stretch applied parallel to long axis of the arm compared to stretch applied perpendicular to the long axis of the arm; the standard error is determined from a least-squares linear fit for each of the trials and the slope and error above is the statistical average of four trials.

Direction of Stretch	Slope
Parallel to long axis of arm	0.0095 ± 0.0002
Perpendicular to long axis	0.0065 ± 0.0008

Note that in our pigskin stretch experiment (Figures 2 and 4), sample shapes before and after the deformation can be approximated with a rectangular geometry. Skin was stretched in one direction (along the grips), and the contraction of the skin, perpendicular to the stretch direction, was prevented by the two metal bars (support rods) (Figure 2). The strain measure ε reflects the deformation along the motion of the grips (Figure 4). On the other hand, in the forearm measurements there was nothing to prevent skin from contracting perpendicular to the direction of the micrometer. The geometry of the skin piece before the deformation (rectangular) distorted after the stretch with the reflectance measured at the center of the initial rectangular region. The definition of strain measure ε at that point can be still used for illustrations (Figures 5 and 6). In both measurements, the grips and the double-sided Scotch tape do not allowed the lateral contraction of the samples during the stretch right next to them. Therefore, for the presented reasons, a simple ideal rectangular geometry that can be used before and after the deformation for computing strain tensors can not be met.[11]

Measurements were repeated with blue light ($\lambda = 488$ nm) from an argon-ion laser. Both wavelengths used in this study gave similar results for the slope, indicating that the applied stretch changes the reflective properties through out the optical penetration depths of the two wavelengths. It is well known that different wavelengths of light penetrate different depths into skin tissue. Previous results with wavelength-dependent polarization imaging show that features below the surface of the skin can be imaged.[18] For a single wavelength, polarization imaging averages over the

Table 2 Measured slope ($\times 10^2$) of reflectivity versus stretch data for human subject 2 on 10 different days; for each day, 10 trials were conducted; the slope for a day is the average of the 10 measurements and the error is determined by the standard deviation of the 10 measurements.

Day 1	Day 2	Day 3	Day 4	Day 5	Day 6	Day 7	Day 8	Day 9	Day 10
1.04 ± 0.09	1.02 ± 0.10	1.02 ± 0.18	1.02 ± 0.18	0.97 ± 0.16	1.01 ± 0.12	1.07 ± 0.15	1.04 ± 0.12	1.02 ± 0.14	1.02 ± 0.08

penetration depth of the light. The imaging of structures at different depths can be achieved by subtracting the normalized polarized reflectivity images (i.e., parallel minus perpendicular polizations) acquired with two different wavelengths (i.e., two different penetration depths). The subtraction will cancel out the image arising from the outer part of the tissue (shorter wavelength image) because the number of photons contributing to this part of the reflectivity is approximately the same for both wavelength images. Therefore, subtracting the two images for different wavelengths produces an image that contains only information from a location in the tissue given by the difference of the penetration depths. This suggests that by using different-wavelength light sources we can map the stretch field of the skin as a function of depth under applied stretch/force.

If one were to measure the absolute reflectivity of skin, the absolute reflectivity would depend on many factors such as age, water content, pigmentation, etc. For all of the measurements on human subjects, care was taken to reproduce the test conditions (e.g., time of day, humidity, test location on the body, skin treatment prior to measurements) for each measurement. However, in our experiments we are mainly concern with the slope of our measurements curves (e.g., the relative change in reflectivity versus change in stretch). For such a measurement, the absolute reflectivity does not matter—only relative changes in slope matter.

The measurements of the deformations and applied loads and estimating the biomechanical properties of tissue are critical to many areas of the health sciences. Measuring the tension in wound closures,[27] skin flaps,[28] and tissue expanders[29] would help surgeons to treat wounds more successfully by minimizing scar tissue and maximizing the speed of treatment, by letting them know how much the skin can be stretched at each treatment step. The measurement techniques, which provide information to the surgeons about the excess mechanical deformations of soft tissue around the surgical site during the surgery, would avoid injury to the surrounding tissue since the optimum amount of force could be applied during suturing.

The noncontact, *in situ* optical technique described in this paper can be easily extended to an imaging technique by replacing the single-element photodetector with a digital CCD (charge-coupled device) camera and using appropriate imaging software to take into account images acquired for different illumination wavelengths. By analyzing the entire reflectivity of the image using a digital camera, the polarization imaging technique can yield the stretch pattern over a large area of tissue. To this end, preliminary measurements of polarization imaging of soft-tissue stretch using a CCD camera demonstrate[30] a lateral spatial resolution of about 25 μm. Moreover, by subtracting polarization images obtained with different wavelengths, corresponding to different optical penetration depths, it is possible to construct a 3-D image[18] of the soft-tissue stretch. Changes in skin stretch properties in an area of interest can be monitored and estimated noninvasively by comparing the reflectivity changes that take place in symmetrical anatomical locations by applying controlled deformations and monitoring the resulting changes that take place in the light reflection properties of the skin.

References

1. T. Gibson, ''Physical properties of skin,'' in *Plastic Surgery*, Vol. 1, *General Principles*, J. G. McCarthy, Ed., pp. 207–220, W. B. Saunders, Philadelphia (1990).
2. C. Cacou, J. M. Anderson, and I. F. K. Muir, ''Measurement of closing force of surgical wound and relation to the appearance of resultant scars,'' *Med. Biol. Eng. Comput.* **32**, 638–642 (1994).
3. C. Cacou and I. F. K. Muir, ''Effects of plane mechanical forces in wound healing in humans,'' *J. R. Coll. Surg. Edinb.* **40**, 38–41 (1995).
4. W. F. Larabee, G. A. Holloway, and D. Sutton, ''Wound tension and blood flow in skin flaps,'' *Ann. Otol. Rhinol. Laryngol.* **93**, 112–115 (1984).
5. H. R. Chaudhry, B. Bukiet, M. Siegel, T. Findley, A. B. Ritter, and N. Guzelsu, ''Optimal patterns for suturing wounds,'' *J. Biomech.* **31**, 653–662 (1998); H. R. Chaudhry, B. Bukeit, T. Findley, and A. B. Ritter, ''Evaluation of residual stress in rabbit skin and the relevant material constants,'' *J. Theor. Biol.* **192**, 191–195 (1998).
6. B. Chretien-Marquet, V. Caillou, D. H. Brasnu, S. Bennaceur, and T. Buisson, ''Description of cutaneous excision and suture using a mathematical model,'' *Plast. Reconstr. Surg.* **103**, 145–150 (1999).
7. D. M. Flynn, G. D. Peura, P. Grigg, and A. H. Hoffma, ''A finite element based method to determine the properties of planar soft tissue,'' *J. Biomed. Eng.* **120**, 202–210 (1998).
8. P. H. DeHoff and J. E. Key, ''Application of the finite element analysis to determine forces and stresses in wound closing,'' *J. Biomech.* **14**, 549–554 (1981).
9. A. Manios, J. Katsantonis, A. Tosca, C. N. Skulakis, and D. Tsiftsis, ''The finite element method adds a research and teaching tool in the analysis of local skin flaps,'' *Dermatol. Surg.* **22**, 1029–1034 (1996).
10. A. Vexler, I. Polyansky, and R. Gorodetsky, ''Evaluation of skin viscoelasticity and anisotropy by measurement of speed of shear wave propagation with viscoelasticity skin analyzer,'' *J. Invest. Dermatol.* **113**, 732–739 (1999).
11. Y. Lanir and Y. C. Fung, ''Two-dimensional mechanical properties of rabbit skin—I. Experimental system,'' *J. Biomech.* **7**, 29–34 (1974); Y. Lanir and Y. C. Fung, ''Two-dimensional mechanical properties of rabbit skin—II. Experimental results,'' *J. Biomech.* **7**, 171–182 (1974).
12. M. Viatour, F. Henry, and G. E. Pierard, ''A computerized analysis of intrinsic forces in the skin,'' *Clin. Exp. Dermatol.* **20**, 308–312 (1995).
13. S. C. Yin, W. R. Tomkins, K. L. Petterson, and M. Intaglietta, ''A video dimension analyzer,'' *IEEE Trans. Biomed. Eng.* **19**, 376–385 (1972).
14. W. P. Smutz, M. Drexler, L. J. Berglund, E. Growney, and K. N. An, ''Accuracy of a video strain measurement system,'' *J. Biomech.* **29**, 813–817 (1996).
15. J. D. Humphrey, ''Mechanics of the arterial wall: review and directions,'' *Crit. Rev. Biomed. Eng.* **23**, 1–162 (1995).
16. R. R. Anderson and J. A. Parrish, ''The optics of human skin,'' *J. Invest. Dermatol.* **77**, 13–19 (1981); R. R. Anderson and J. A. Parish, ''Optical properties of human skin,'' Chap. 6 in *The Science of Photomedicine*, J. D. Regan and J. A. Parrish, Eds., pp. 147–194, Plenum, New York (1982).
17. J. F. Federici, N. Guzelsu, H. C. Lim, G. Jannuzzi, T. Findley, H. R. Chaudhry, and A. B. Ritter, ''Non-invasive light reflection technique for measuring soft-tissue stretch,'' *Appl. Opt.* **38**, 6653–6660 (1999).
18. S. G. Demos and R. R. Alfano, ''Optical polarization imaging,'' *Appl. Opt.* **36**, 150–155 (1997).
19. R. R. Anderson, ''Polarized light examination and photography of the skin,'' *Arch. Dermatol.* **127**, 1000–1005 (1991).
20. E. Fariza, T. O'Day, A. E. Jalkh, and A. Medina, ''Use of cross-polarized light in anterior segment photography,'' *Arch. Ophthalmol. (Chicago)* **107**, 608–610 (1989).
21. J. Philp, N. J. Carter, and C. P. Lenn, ''Improved optical discrimination of skin with polarized light,'' *J. Soc. Cosmet. Chem.* **39**, 121–132 (1988).
22. S. L. Jacques, J. R. Roman, and K. Lee, ''Imaging superficial tissues with polarized light,'' *Lasers Surg. Med.* **26**, 119–129 (2000).
23. M. B. Ostermeyer, D. V. Stephensen, L. Wang, and S. L. Jacques, ''Nearfield polarization effects on light propagation in random media,'' in *OSA TOPS on Biomedical Optical Spectroscopy and Diagnostics*, E. Sevick-Muraca and D. Benaron, Eds., Vol. 3, pp. 20–25, Optical Society of America, Washington, D.C. (1996).

24. R. Reihsner, B. Balogh, and E. J. Menzel, ''Two dimensional elastic properties of human skin in terms of an incremental model at the *in-vivo* configuration,'' *Med. Eng. Phys.* **17**, 304–313 (1995).
25. J. Ferguson and J. C. Barbenel, ''Skin surface patterns and the directional mechanical properties of the dermis,'' in *Bioengineering and the Skin*, R. Marks and P. A. Payne, Eds., pp. 83–92, MTP, Lancaster (1981).
26. S. Makki, J. C. Barbenel, and P. Agache, ''A quantitative method for the assessment of the microtopography of human skin,'' *Acta Derm Venereol* **59**, 285–291 (1979).
27. E. E. Peacock, Jr. and I. K. Cohen, ''Wound healing,'' Chap. 5 in *Plastic Surgery*, Vol. 1. *General Principles*, J. G. McCarthy, Ed., pp. 161–181, W. B. Saunders, Philadelphia (1990).
28. R. K. Daniel and C. L. Kerrigan, ''Principles and physiology of skin flap surgery,'' Chap. 9 in *Plastic Surgery*, Vol. 1, *General Principles*, J. G. McCarthy, Ed., pp. 275–328, W. B. Saunders, Philadelphia (1990).
29. L. C. Argenta and E. D. Austad, ''Principles and techniques of tissue expansion,'' Chap. 13 in *Plastic Surgery*, Vol. 1, *General Principles*, J. G. McCarthy, Ed., pp. 475–507, W. B. Saunders, Philadelphia (1990).
30. B. Schulkin, H. C. Lim, G. Jannuzzi, J. F. Federici, and N. Guzelsu, ''Spatial and stretch resolution of soft-tissue stretch by polarization imaging'' (in preparation).